

RESEARCH

Open Access



Alkaline-enhanced boehmite catalysts for catalytic hydrolysis of carbonyl sulfide at low temperature

Jia-Yin Lin^{1,2*}, Jia-Yu Lee¹ and Chih-Ying Wang¹

Abstract

The removal of carbonyl sulfide (COS), a byproduct gas in the steel industry, is crucial due to its environmental impact, including acid rain formation and corrosion of chemical equipment. This study explores enhancing the catalytic performance for COS hydrolysis at low temperatures by loading potassium hydroxide (KOH) onto boehmite catalysts. The modified catalysts demonstrated significantly improved COS conversion rates and hydrogen sulfide (H₂S) yields compared to untreated counterparts. At 40 °C, K/Boehmite catalysts achieved approximately 80% COS conversion. As the temperature increased to 50, 60, and 70 °C, COS conversion efficiencies neared 100%, with H₂S yields reaching up to 98% for K/Boehmite-3 (A method involving the loading of KOH onto boehmite catalysts.) Characterization results confirmed that KOH increased the number of active sites on the catalyst surface, enhancing COS adsorption and reaction. The KOH modification increases alkalinity and promotes the formation of surface hydroxyl groups, which play a key role in the hydrolysis reaction. These hydroxyl groups facilitate water adsorption and the breakdown of COS into H₂S and CO₂. This study presents a straightforward method for KOH impregnation on boehmite, marking the first use of boehmite as a COS hydrolysis catalyst, significantly boosting its efficiency and offering a viable solution for industrial COS removal while effectively generating H₂S.

Keywords Carbonyl sulfide, Hydrogen sulfide, Catalytic hydrolysis, Boehmite, Alkali metal

1 Introduction

Carbonyl sulfide (COS) is a prevalent byproduct gas in the steel industry, notably present in blast furnace gas, coke oven gas, and converter gas [1]. The environmental issues associated with COS emissions, including acid rain formation and the consequential corrosion of chemical equipment, have attracted extensive attention in recent years [2, 3]. To date, adsorption [4], hydrogenation conversion [5], and hydrolysis [6] methods are widely

employed for COS removal in the industry. Among these methods, hydrolysis has been the most widely used technology due to its mild operating conditions and high conversion efficiency [7]. Besides, with the growing attention toward circular economy and sustainability, the product hydrogen sulfide (H₂S) after the hydrolysis reaction can be utilized in industrial processes. However, hydrolyzing COS without a catalyst would be difficult. Hence, the selection of adequate catalysts holds paramount importance for the effective catalytic hydrolysis of COS. On the other hand, the cost-effectiveness and ease of preparation of catalysts are crucial issues in industrial applications. The hydrolysis reaction equations are displayed as follows ((Eq. (1) is the main reaction, Eqs. (2) and (3) are the main side reactions) [8].

*Correspondence:

Jia-Yin Lin

joylin7@dragon.nchu.edu.tw

¹ Semiconductor and Green Technology Program, National Chung Hsing University, Nantou 540001, Taiwan

² Industrial and Smart Technology Program, National Chung Hsing University, Nantou 540001, Taiwan



© The Author(s) 2025. **Open Access** This article is licensed under a Creative Commons Attribution 4.0 International License, which permits use, sharing, adaptation, distribution and reproduction in any medium or format, as long as you give appropriate credit to the original author(s) and the source, provide a link to the Creative Commons licence, and indicate if changes were made. The images or other third party material in this article are included in the article's Creative Commons licence, unless indicated otherwise in a credit line to the material. If material is not included in the article's Creative Commons licence and your intended use is not permitted by statutory regulation or exceeds the permitted use, you will need to obtain permission directly from the copyright holder. To view a copy of this licence, visit <http://creativecommons.org/licenses/by/4.0/>.

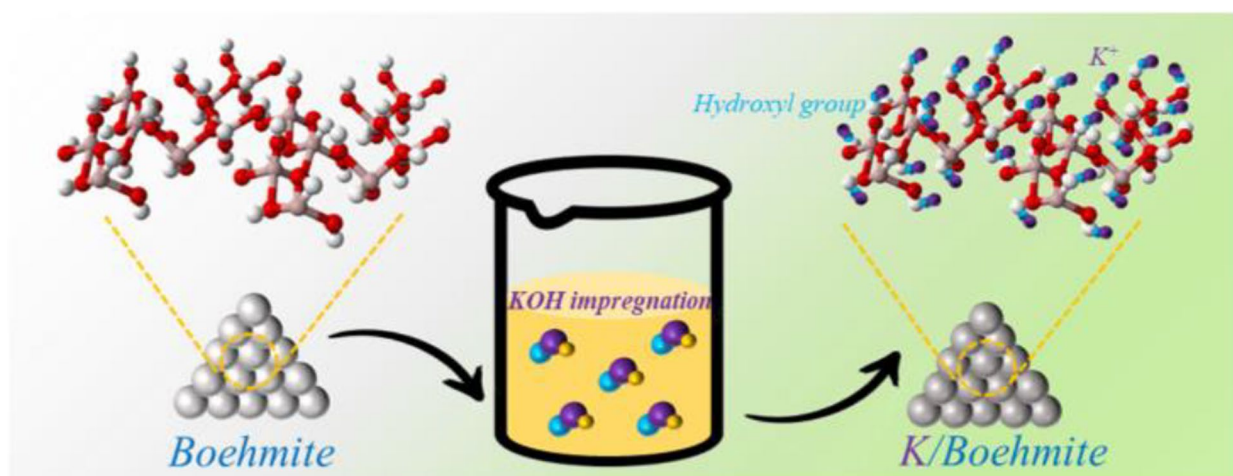


Fig. 1 Schematic process for the fabrication of K/Boehmite materials



Current studies have focused on carbon-based, aluminum-based and metal oxide as catalyst carriers [7–11]. Among these materials, boehmite (AlO(OH)) as a supported metal stands out as a promising choice due to its excellent thermal stability and large surface area. Additionally, boehmite exhibits favorable hydrophilic properties [12], allowing it to adsorb water molecules and promote the contact between water and COS, thereby increasing the reaction conversion and selectivity. Moreover, boehmite can partially facilitate the hydrolysis of COS. The catalytic hydrolysis of COS is a base-catalyzed reaction [13]. The introduction of alkali metals [14], rare earth metals [15], and transition metals [16] as active sites can enhance COS removal. Therefore, the alkalinity of the hydrolysis catalyst will play an important role in enhancing catalytic efficiency. Potassium ions in potassium hydroxide (KOH) used as active metal loaded on supported catalysts have several advantages. Firstly, the K^+ ions serve as an efficient base catalyst is not only enhancing the alkalinity of the catalyst but also increasing the concentration of water molecules on the catalyst surface, further accelerating the hydrolysis reaction [11, 17].

Secondly, the OH^- ions can improve the surface hydroxyl group amount on boehmite. These hydroxyl groups promote water adsorption and facilitate the hydrolysis reaction of COS, dissociating to H_2S and CO_2 . Most importantly, KOH is a widely available and

relatively inexpensive chemical reagent readily accessible in the market.

In this work, three different size boehmite materials were chosen as the catalyst carrier and loaded alkali ions as active site on it through impregnation method under ambient temperature. The removal of COS via catalytic hydrolysis and H_2S yield were examined, also, catalytic stability of catalyst was evaluated. Moreover, the reaction and deactivation mechanisms of COS catalytic hydrolysis were explored to confirm the influence of alkali metals and alkali ions in the reaction.

2 Materials and methods

2.1 Reagents and chemicals

The chemicals used in this work were available technical-grade materials and were used as obtained without further purification. Boehmite-1 (3–5 mm) and KOH were purchased from Emperor Chemical (Taiwan). Boehmite-2 (5–7 mm) was received from Kidays-Global Co. (Taiwan). Boehmite-3 (1.5–3 mm) was purchased from EIKME (Taiwan). Deionized (DI) water was used for aqueous solutions.

2.2 Preparation and characterization of K/Boehmite

The preparation of the process for K/Boehmite can be depicted in Fig. 1. A series of three K/Boehmite materials was immersed into a concentration of 20 g L^{-1} for 72 h at room temperature. Next, the resulting product was collected via filtration, washed with DI water several times, and dried at $80 \text{ }^\circ\text{C}$ in an oven to acquire K/Boehmite-1, K/Boehmite-2 and K/Boehmite-3. In this work, the R-ray Powder Diffraction pattern of all as-prepared catalysts was investigated by an X-ray diffractometer (XRD, Bruker, USA). Morphologies of boehmite materials and

all as-prepared catalysts were characterized by a scanning electron microscope (SEM, JOEL, Japan). Thermogravimetric analysis (TGA) of all as-prepared catalysts were measured by a TGA analyzer (TGA 4000, PerkinElmer, USA). The specific surface area and pore size distribution of the catalyst were determined by a gas adsorption analyzer (NOVAtouch, Anton Paar, Austria). The CO₂ temperature-programmed desorption (CO₂-TPD) was carried out to estimate the surface basicity of catalyst using chemisorption analyzer (ASIQ TPx, Anton Paar, Austria). Before conducting adsorption measurement, all samples were firstly degassed at 400 °C for 1 h, then the sample was exposed in 20 mL min⁻¹ of 5% CO₂/N₂ at 25 °C for 1 h and then was purged by N₂ in a heating program from 25 to 800 °C with heating rate of 10 °C min⁻¹. Furthermore, Fourier Transform Infrared Spectroscopy (FT-IR) (iS5, Thermo Fisher Scientific) was used for identifying of gaseous products. To verify the catalytic scheme, X-ray photoelectron spectroscopy (XPS) (PHI 5000 ULVAC-PHI, Japan) was applied to investigate the valence states of active surface elements.

2.3 Catalytic activity measurement

The tubular fixed-bed reactor equipped with a heating device was employed to replicate the activity and H₂S yield of the catalysts. Typically, the total gas flow rate was 500 mL min⁻¹ (balanced by N₂), achieved by premixing in a gas mixer to produce a simulated gas containing 100 ppm of COS and a specified amount of water vapor (7.28%), which was controlled by passing N₂ through a water reservoir maintained at 40 °C. 1 g of catalyst and the mixed gas was introduced into a quartz tube, H₂S concentrations were continually monitored by a gas detector (POLI MP400P) and the concentration of COS were analyzed by FY-IR spectrophotometer, Figs. S1a and S1b displays the FY-IR spectra of COS and calibration curves, respectively.

The COS conversion and H₂S yield were calculated by:

$$\text{COS conversion} = \frac{[\text{COS}]_{\text{in}} - [\text{COS}]_{\text{out}}}{[\text{COS}]_{\text{in}}} \times 100\%$$

$$\text{H}_2\text{S yield} = \frac{[\text{H}_2\text{S}]_{\text{out}}}{[\text{COS}]_{\text{in}} - [\text{COS}]_{\text{out}}} \times 100\%$$

3 Results and discussion

3.1 Characterization of boehmite and K/Boehmite materials

In order to examine the crystalline structure of the boehmite materials, XRD analysis was conducted, and the resulting patterns are shown in Fig. 2a. The significant peaks observed at 14, 28, 38, 49, and 67° 2θ are indexed

and assigned to the orthorhombic phase of boehmite (AlO(OH)). Specifically, the peaks correspond to the (020), (120), (140), (200), and (231) planes, respectively, which are characteristic of orthorhombic boehmite. These indexed peaks confirm the presence of the orthorhombic AlO(OH) crystalline phase in all three samples (boehmite-1, boehmite-2, and boehmite-3). The indexing of these peaks enhances the clarity of the structural characterization, providing a clear confirmation of the crystalline phases present in the samples.

The N₂ adsorption isotherm and pore size distribution spectra are illustrated in Fig. 2b and c, respectively, and the textural properties of boehmite are presented in Table 1. The adsorption isotherms exhibited by all boehmites conform to the IUPAC type IV isotherm, suggesting that comprised porous structures. The pore size distribution, as depicted in Fig. 2c, further confirms that all boehmites contain pores ranging from a few nanometers to mesoporous. The surface area of boehmite-1 and boehmite-3 is 312 and 321 m² g⁻¹, respectively. Boehmite-2 exhibits a slightly lower surface area at 219 m² g⁻¹, which is slightly below the other two. On the other hand, total pore volume of boehmite-1, boehmite-2 and boehmite-3 are 0.36, 0.40 and 0.46 mL g⁻¹, respectively. After KOH impregnation, the surface area of K/Boehmite-1, K/Boehmite-2, and K/Boehmite-3 decreased to 256, 186, and 267 m² g⁻¹, respectively, as shown in Fig. 2d and e. This reduction in surface area is consistent with the expectation that KOH loading could partially block the pores or cover the surface, leading to a lower accessible surface area. The decrease is most pronounced in K/Boehmite-2, likely due to its initially lower surface area and pore volume, which makes it more susceptible to pore blockage during KOH impregnation. Despite this reduction, K/Boehmite-3 maintained a relatively higher surface area and pore volume, suggesting that its larger pores were less affected by the KOH loading. These findings underscore the impact of KOH impregnation on the textural properties of boehmite materials, which is crucial for understanding their catalytic performance.

The morphologies of boehmite materials and the as-prepared catalyst were observed through SEM as displayed in Fig. 3. Figure 3a–c depicts the SEM image of boehmite materials, characterized by irregular shapes and some surfaces displaying a flaky structure. After KOH impregnation, the catalyst retains a similar appearance to the original as exhibited in Fig. 3d–f. To further investigate the elemental composition, Energy dispersive spectrometer (EDS) analysis was employed for identification as displayed in Fig. S2. Figures S2a–S2c reveals that the prominent elements on boehmite materials before KOH impregnation, revealing that the prominent elements are aluminum (Al) and oxygen

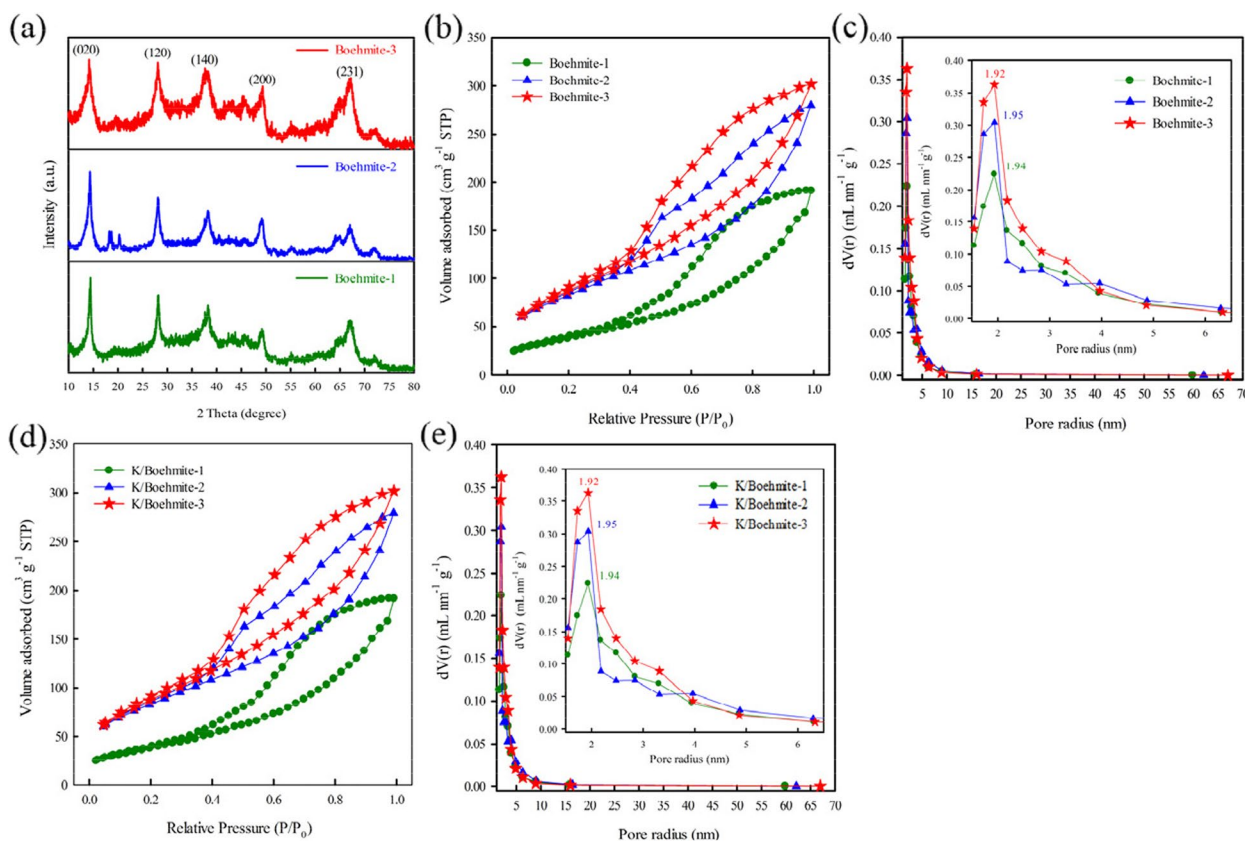


Fig. 2 a XRD pattern, b N₂ sorption isotherm, and c pore size distribution of Boehmite materials; d N₂ sorption isotherm, and e pore size distribution of K/Boehmite materials

Table 1 Textural properties of boehmite materials

| | Surface area (m ² g ⁻¹) | Pore Volume (mL g ⁻¹) |
|--------------|------------------------------------------------|-----------------------------------|
| Boehmite-1 | 312 | 0.36 |
| Boehmite-2 | 220 | 0.41 |
| Boehmite-3 | 321 | 0.46 |
| K/Boehmite-1 | 256 | 0.34 |
| K/Boehmite-2 | 186 | 0.26 |
| K/Boehmite-3 | 267 | 0.42 |

(O) with weight percentages of Al – 45.6, 46.7, and 46.9, and O – 54.4, 53.4, and 53.1%, respectively. On the other hand, Figs. S2d–S2f shows the spectrum of the as-prepared K/Boehmite materials, in addition to the original Al and O element, the presence of potassium (K) is clearly observed. The weight percentages of potassium are 3.44, 3.08, and 5.30% as displayed in Fig. 3d–f, respectively. This evidence proves that the simple impregnation method can effectively dope alkali metal onto boehmite materials, significantly increasing

the potassium content and enhancing the catalytic properties of the boehmite for the catalytic hydrolysis of COS.

To examine the influence of alkaline sites on the catalysts and after KOH impregnation method, CO₂-TPD was utilized to analyze the distribution of alkaline centers, and exhibited in Fig. 4a and b. Typically, the strength of basic site is classified into three categories, weak (<200 °C), medium (200–500 °C) and strong (>500 °C) [18]. The weak basic site is associated with CO₂ species adsorbed onto surface hydroxyl groups with weak bonding. the medium basic sites are attributed to adsorption over metal oxygen pairs, such as Al-O. Conversely, high-temperature desorption peaks (>500 °C) are linked to coordinatively unsaturated O²⁻ groups resulting from the partial breakdown of metal–oxygen pairs [19]. Obviously, the majority of basic sites observed in boehmite materials predominantly comprise strong basic sites, with only partial presence of weak sites, and notably lacking any discernible weak basic sites. However, the boehmite material after the KOH impregnation method indicates significant promotion of weak and medium basic sites, benefiting the catalytic hydrolysis reaction.

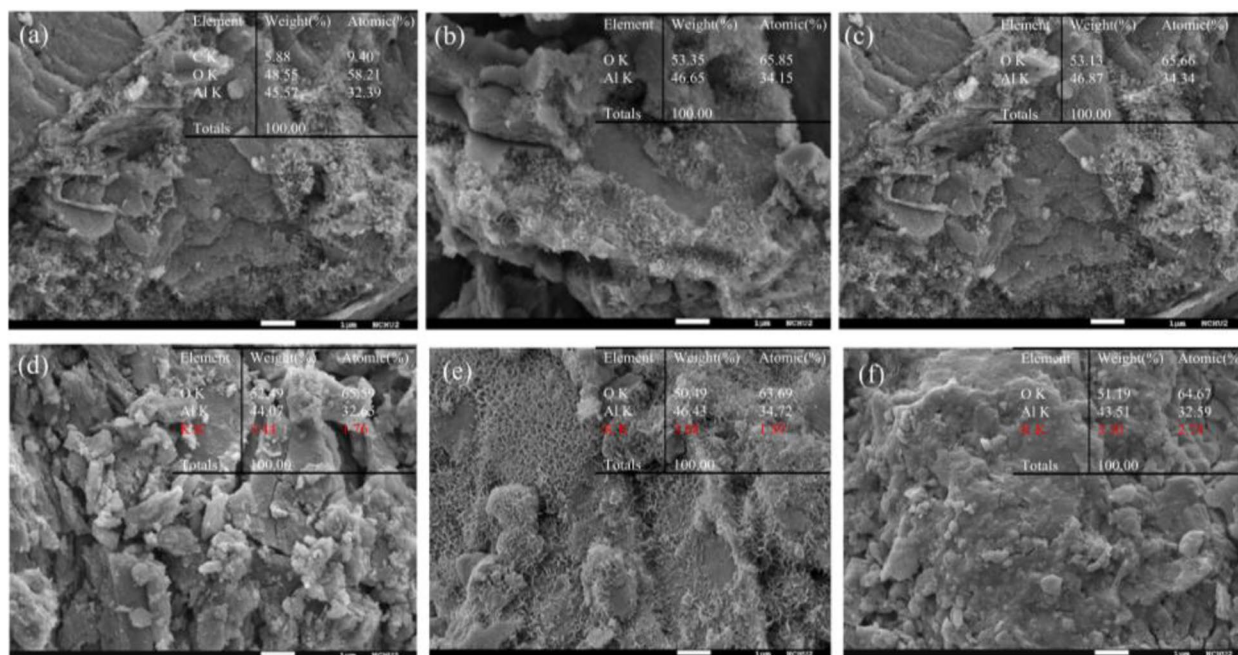


Fig. 3 SEM image of a Boehmite-1, b Boehmite-2, c Boehmite-3, d K/Boehmite-1, e K/Boehmite-2 and f K/Boehmite-3

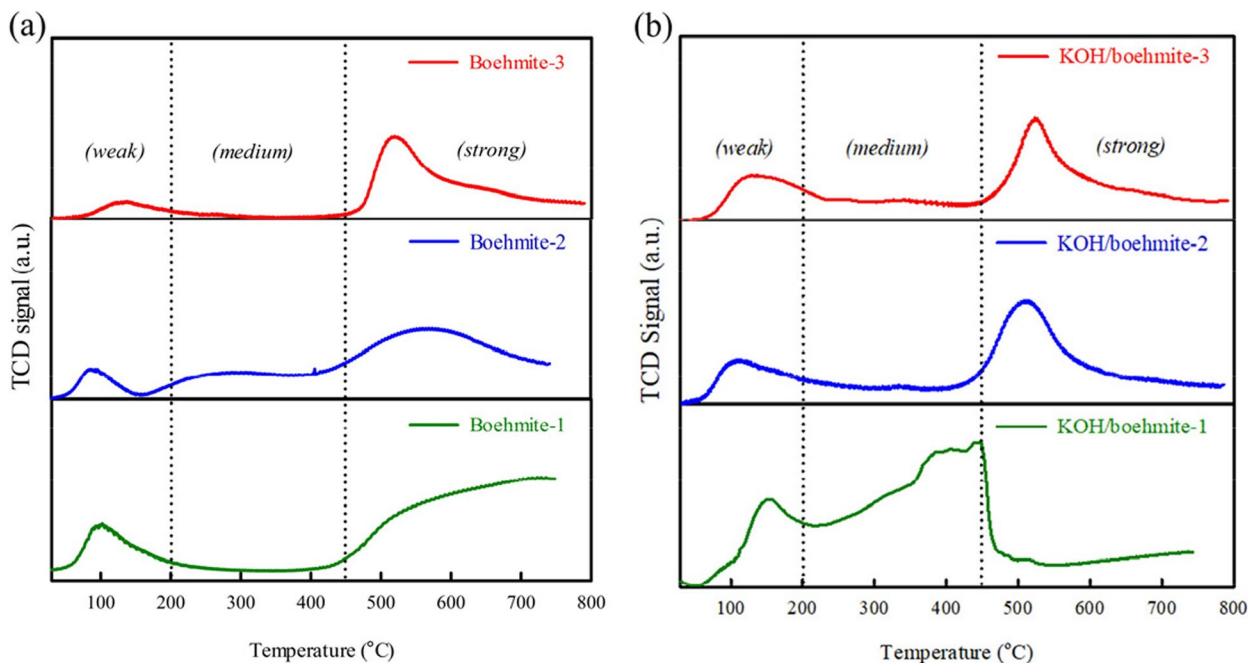


Fig. 4 CO₂-TPD profiles of a the Boehmite-1, Boehmite-2 and Boehmite-3, b K/Boehmite-1, K/Boehmite-2 and K/Boehmite-3

During the reaction process, the thermal stability of catalyst is a critical issue. Hence, Fig. 5a–b present the TGA curve for the as-prepared catalysts and after KOH impregnation method, respectively. The thermogravimetric curve exhibits two mass loss features at

100 and 400 °C. The initial mass loss observed at 100 °C can be attributed to the departure of water molecules from the boehmite. Following this, a significant mass loss occurred at 400 °C, indicating the transformation of AlO(OH) to γ -Al₂O₃ phase [20]. After the

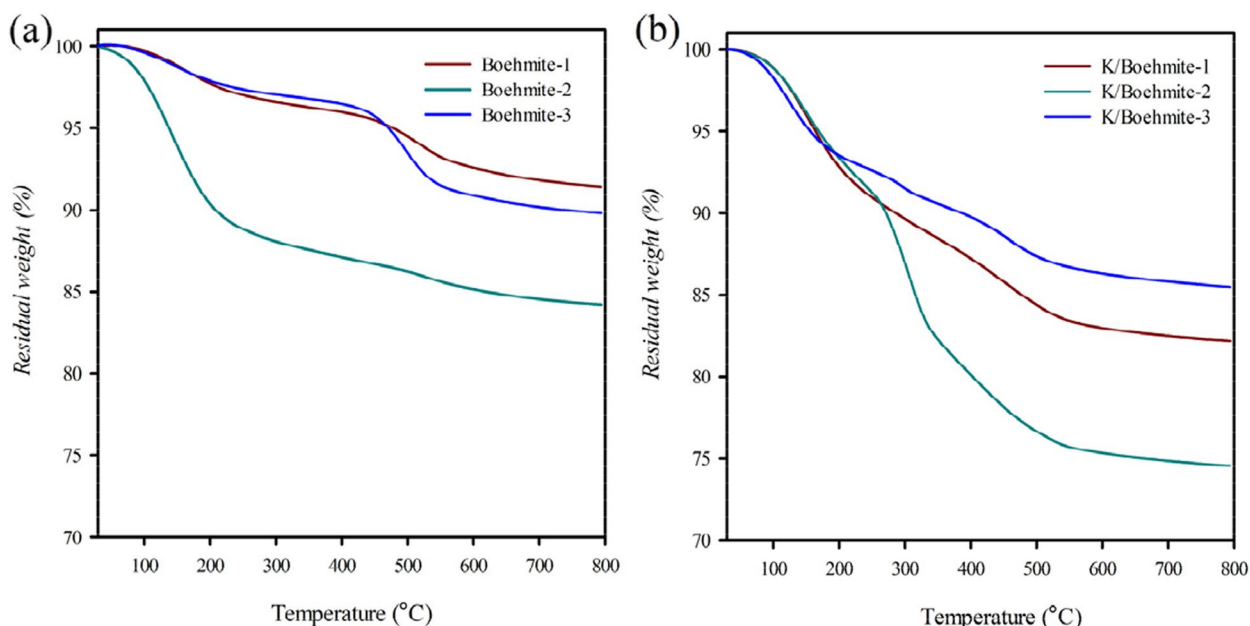


Fig. 5 TGA curves of **a** the Boehmite-1, Boehmite-2 and Boehmite-3, **b** K/Boehmite-1, K/Boehmite-2 and K/Boehmite-3 under air atmosphere

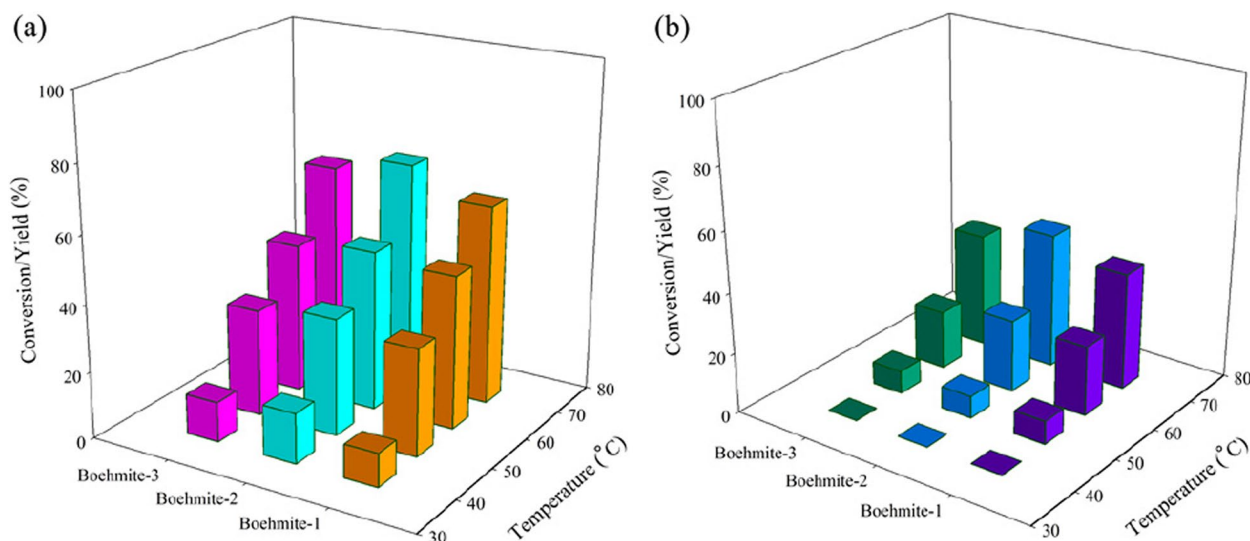


Fig. 6 Catalytic hydrolysis **a** conversion of COS and **b** H₂S yield using Boehmite-1, Boehmite-2 and Boehmite-3 at different temperatures. ([COS] = 100 ppm, Gas Hourly Space Velocity = 5834 h⁻¹, water vapor = 7.28%)

KOH impregnation method, an increase in mass loss is observed in the as-prepared catalysts compared to the pristine boehmite, which can be attributed to the addition of KOH. Although this increase in mass loss, the impregnated catalyst reveals excellent thermal stability even at elevated temperatures, indicating its suitability for not only low-temperature but also high-temperature applications.

3.2 Effect of temperature on COS removal and H₂S yield

To investigate the effect of temperature on COS removal, COS conversion and H₂S yield were measured at different temperatures. As shown in Fig. 6, COS conversion results are depicted in Fig. 6a, while H₂S yield results are illustrated in Fig. 6b. The COS conversion and H₂S yield for all three materials were low (below 10%) at 40 °C. For boehmite-1, the COS conversion efficiency at 50, 60, and 70 °C were approximately 30, 50, and 80%,

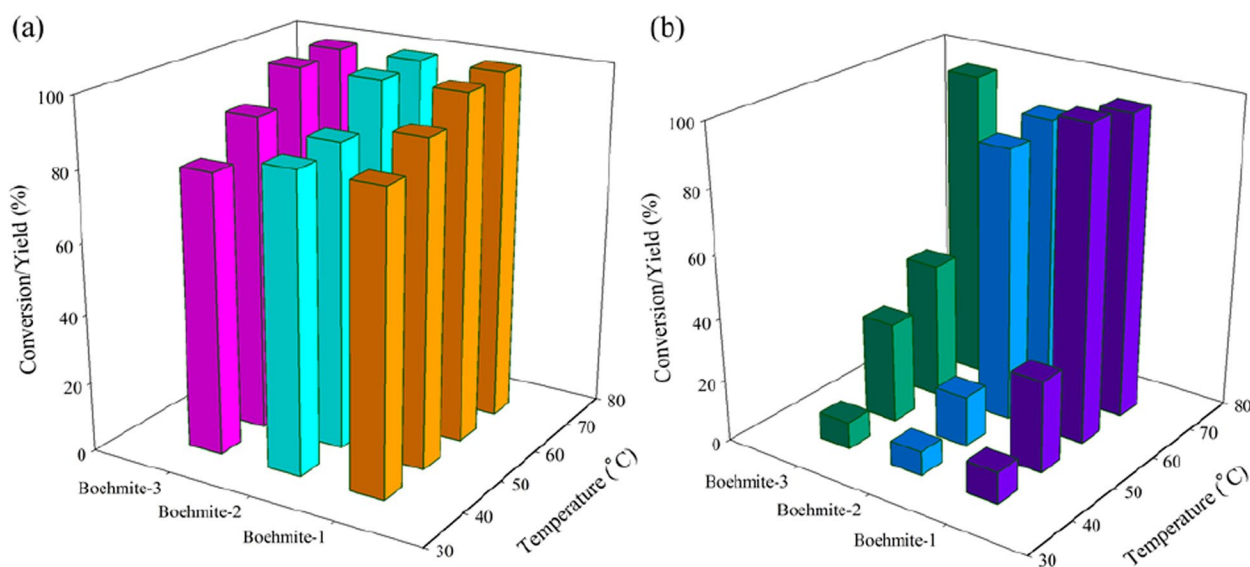


Fig. 7 Catalytic hydrolysis **a** conversion of COS and **b** H₂S yield using K/Boehmite-1, K/Boehmite-2 and K/Boehmite-3 at different temperatures. ([COS] = 100 ppm, Gas Hourly Space Velocity = 5834 h⁻¹, water vapor = 7.28%)

respectively, while the H₂S yields were 15, 25, and 45%. Boehmite-2 and boehmite-3 exhibited similar behavior to boehmite-1, with both COS conversion and H₂S yield significantly increasing with temperature. The increase in temperature promotes the adsorption of COS on the catalyst surface and accelerates the reaction rate, thereby enhancing COS conversion efficiency and H₂S production. This indicates that temperature has a crucial impact on the catalytic hydrolysis of COS.

3.3 Effect of K/Boehmite catalysts on COS removal and H₂S yield

To estimate the effect of alkali metal loading on boehmite for COS removal and H₂S yield, the COS conversion and H₂S yield were measured for K/Boehmite-1, K/Boehmite-2, and K/Boehmite-3 at different temperatures. The results are shown in Fig. 7, COS conversion results are exhibited in Fig. 7a, while H₂S yield results are illustrated in Fig. 7b. K/Boehmite catalysts exhibited higher COS conversion and H₂S yield at all tested temperatures. As the temperature increased, both COS conversion and H₂S yield for K/Boehmite materials significantly improved. At 40 °C, the COS conversion for K/Boehmite-1, K/Boehmite-2, and K/Boehmite-3 was approximately 80%, with H₂S yields around 5–10%. When the temperature was raised to 50 °C, the COS conversion for all three materials approached nearly 100%, with H₂S yields increasing to approximately 29, 16, and 32%, respectively. At further elevated temperatures of 60 and 70 °C, the COS conversion and H₂S yield for K/Boehmite-1 were both close to 100%. For K/Boehmite-2, the

H₂S yields were 87 and 90% at 60 and 70 °C, respectively, while for K/Boehmite-3, the H₂S yields were 44 and 98%, respectively.

The superior performance of K/Boehmite-1 can be attributed to its optimal potassium loading, which enhance catalyst to be more alkaline and increases the number of active sites available for COS adsorption and hydrolysis. Additionally, K/Boehmite-1's high surface area and well-defined pore structure facilitate greater diffusion and interaction of COS molecules with these active sites. The KOH modification also significantly boosts the number of surface hydroxyl groups, which are crucial for the hydrolysis reaction by promoting water adsorption. These factors synergistically contribute to the enhanced catalytic efficiency observed with K/Boehmite-1. This indicates that the introduction of alkali metal increases the number of active sites on the catalyst surface, promoting the adsorption and reaction rate of COS, thereby enhancing the conversion efficiency of COS and the yield of H₂S. Additionally, higher temperatures further enhance the activity of these sites, making it easier for COS to react on the catalyst surface to form H₂S. Table 2 summarizes a literature review and performance comparison across different studies. As shown in Table 2, the K/Boehmite-1 catalyst exhibits the best COS hydrolysis performance at low temperatures compared to other catalysts. The novelty of this study lies in the use of boehmite as catalyst support, which has not been extensively explored in previous studies. Furthermore, the K/Boehmite-1 catalyst not only achieves 100% COS conversion but also reaches a 100% H₂S yield at 60 °C,

Table 2 Studies of catalytic conversion of COS to H₂S over various catalysts

| Catalyst | Reaction temperature (°C) | COS Conversion (%) | H ₂ S Yield (%) | Ref |
|---------------------------|---------------------------|--------------------|----------------------------|-----------|
| K/Boehmite-1 | 60 | 100 | 100 | This work |
| NH ₃ -Fe/MCSAC | 50 | 93.5 | - | [10] |
| Fe-Cu-KOH/WSB | 70 | 70 | - | [16] |
| 10-KA | 50 | 90 | 80 | [7] |
| MgAlCeOx | 50 | 70 | - | [21] |
| ZnAl-20Sm-Na MMO | 60 | 90 | 50 | [22] |

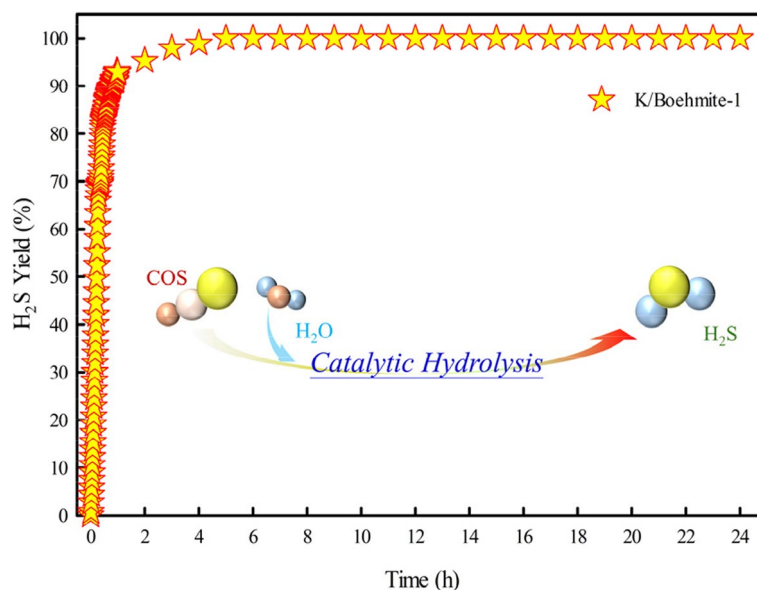


Fig. 8 Durability performance of COS hydrolysis on K/Boehmite-1 ([COS]= 100 ppm, Gas Hourly Space Velocity = 5834 h⁻¹, water vapor = 7.28%, temperature = 60 °C)

demonstrating superior catalytic efficiency under milder conditions than those used in previous works. These results demonstrated the effectiveness of KOH impregnation on boehmite, offering a viable and highly efficient solution for industrial COS removal.

3.4 Durability performance

The durability of the K/Boehmite-1 catalyst for COS hydrolysis was evaluated in the presence of 100 ppm COS. As shown in Fig. 8, the concentration of H₂S produced by the K/Boehmite-1 catalyst rapidly increased and stabilized at around 100 ppm within the first hour of the reaction. This high level of H₂S production was maintained consistently over the entire 24-h testing period. The stability and sustained performance of the K/Boehmite-1 catalyst indicate its excellent catalytic durability for the hydrolysis of COS. Unlike other catalysts which may exhibit a decline in activity over time, K/Boehmite-1 maintained near 100% efficiency, demonstrating

its potential for industrial applications. This consistent performance underscores the robustness of the KOH impregnation method in enhancing the catalytic properties of boehmite for effective and durable COS removal.

3.5 Surface chemistry by XPS

To explore the mechanism of the COS catalytic hydrolysis reaction, we analyzed the chemical state changes on the surface elements of the catalysts using XPS. The XPS survey spectra shown in Fig. 9 exhibit distinct peaks corresponding to Al and O elements in the upper spectrum for boehmite-1, which are characteristic of the AlO(OH) structure (Fig. 9a). The main peaks observed are Al 2p, Al 2s, O 1s, and minor peaks associated with surface hydroxyl groups. Besides, the lower spectrum for the used boehmite-1 catalyst shows a decrease in the intensity of the Al and O peaks, indicating changes in the surface composition after the catalytic reaction. Additionally, new peaks corresponding

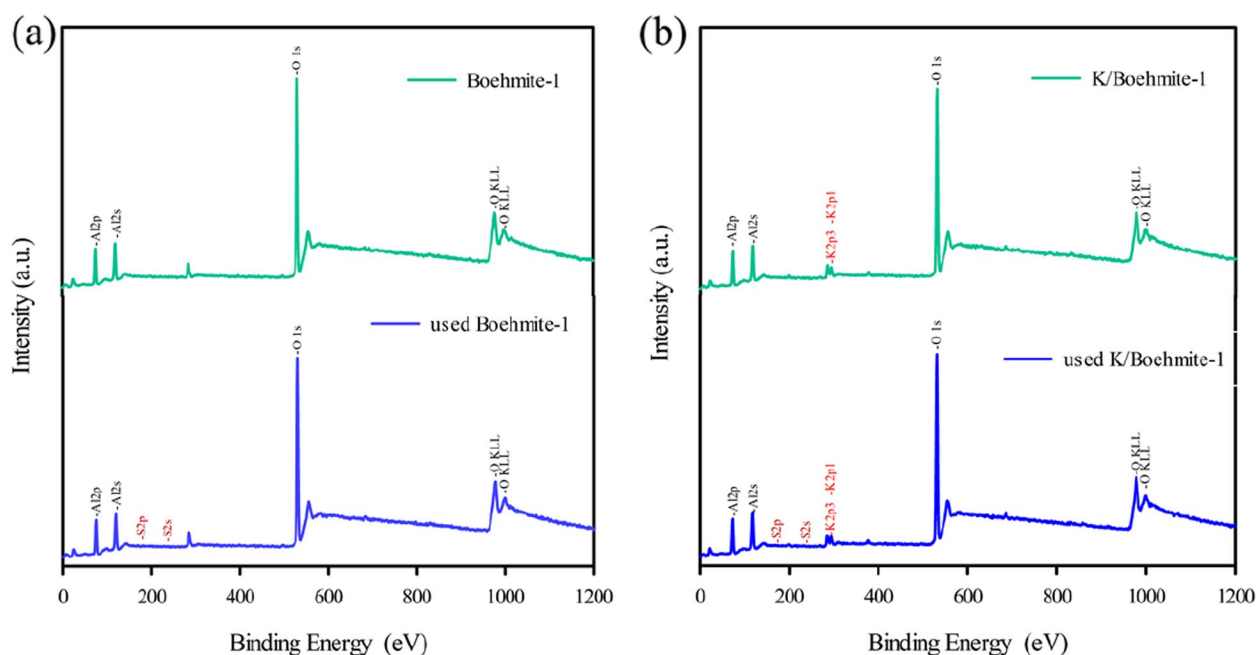


Fig. 9 XPS survey spectra of **a** fresh Boehmite-1 and used Boehmite-1, **b** fresh K/Boehmite-1 and used K/Boehmite-1

to sulfur (S) are observed, suggesting the adsorption of sulfur-containing species, likely reaction products or intermediates, on the catalyst surface. Figure 9b illustrates the upper spectrum for the fresh K/Boehmite-1 catalyst displays similar Al and O peaks as seen in the fresh boehmite-1 spectrum, along with additional peaks corresponding to potassium (K) from the KOH loading. The presence of K is confirmed by the K 2p and K 2s peaks, indicating successful impregnation of KOH onto the boehmite. And the lower spectrum for the used K/Boehmite-1 catalyst shows reduced intensity in the Al and O peaks, similar to the used boehmite-1 catalyst, but with a noticeable retention of the K peaks. Furthermore, significant peaks corresponding to S appear, indicating that sulfur-containing species have adsorbed onto the catalyst surface during the reaction. This observation suggests that the catalyst effectively participates in the hydrolysis of COS, leading to the formation and adsorption of sulfur-containing products like H_2S on the catalyst surface.

As shown in Fig. 10, the O 1s spectrum can be decomposed into three types of oxygen species. The peaks at approximately 530.0, 532.1, and 533.2 eV correspond to bulk oxygen from the crystal structure (Al-O), surface hydroxyl groups (Al-OH), and adsorbed water on the surface (H-OH), respectively [23]. The properties of the catalysts are detailed in Table 3. Among these oxygen species, surface-OH groups play a crucial role in the reaction by facilitating the activation

of COS adsorbed on the catalyst surface, which then reacts with H_2O to produce H_2S .

Table 3 shows that the H-OH ratio in boehmite decreases from 25.5 to 19.2% after the catalytic hydrolysis reaction. Additionally, the H-OH ratio in boehmite increases from 25.5 to 30.1% after immersion with KOH. The introduction of alkali metal hydroxide significantly impacts the catalysts, as evident from the increase in the Al-O ratio after the catalytic hydrolysis reaction, shown in Fig. 10b and d. The shift of the O 1s peaks to higher binding energy in the used K/Boehmite sample indicates electron transfer from the O 1s orbital.

Through examining various physical and chemical parameters, it is evident that alkali metals play a pivotal role in the COS catalytic hydrolysis reaction. During the reaction, the competitive adsorption of COS and H_2O notably affects the efficiency of COS removal, particularly for Al-based catalysts due to the strong water adsorption capacity of $\text{AlO}(\text{OH})$. H_2O readily adsorbs on the catalyst surface, inhibiting COS adsorption. Modification with alkali metal hydroxide enhances COS adsorption. Potassium ions in the catalytic process render catalyst more alkaline. The surface hydroxyl groups (-OH) promote water adsorption and reaction, serving as crucial active sites for the hydrolysis reaction. These hydroxyl groups help break down COS molecules, resulting in the formation and dissociation of H_2S and CO_2 . Therefore, we propose a catalytic mechanism illustrated in Fig. 11. The strong interaction

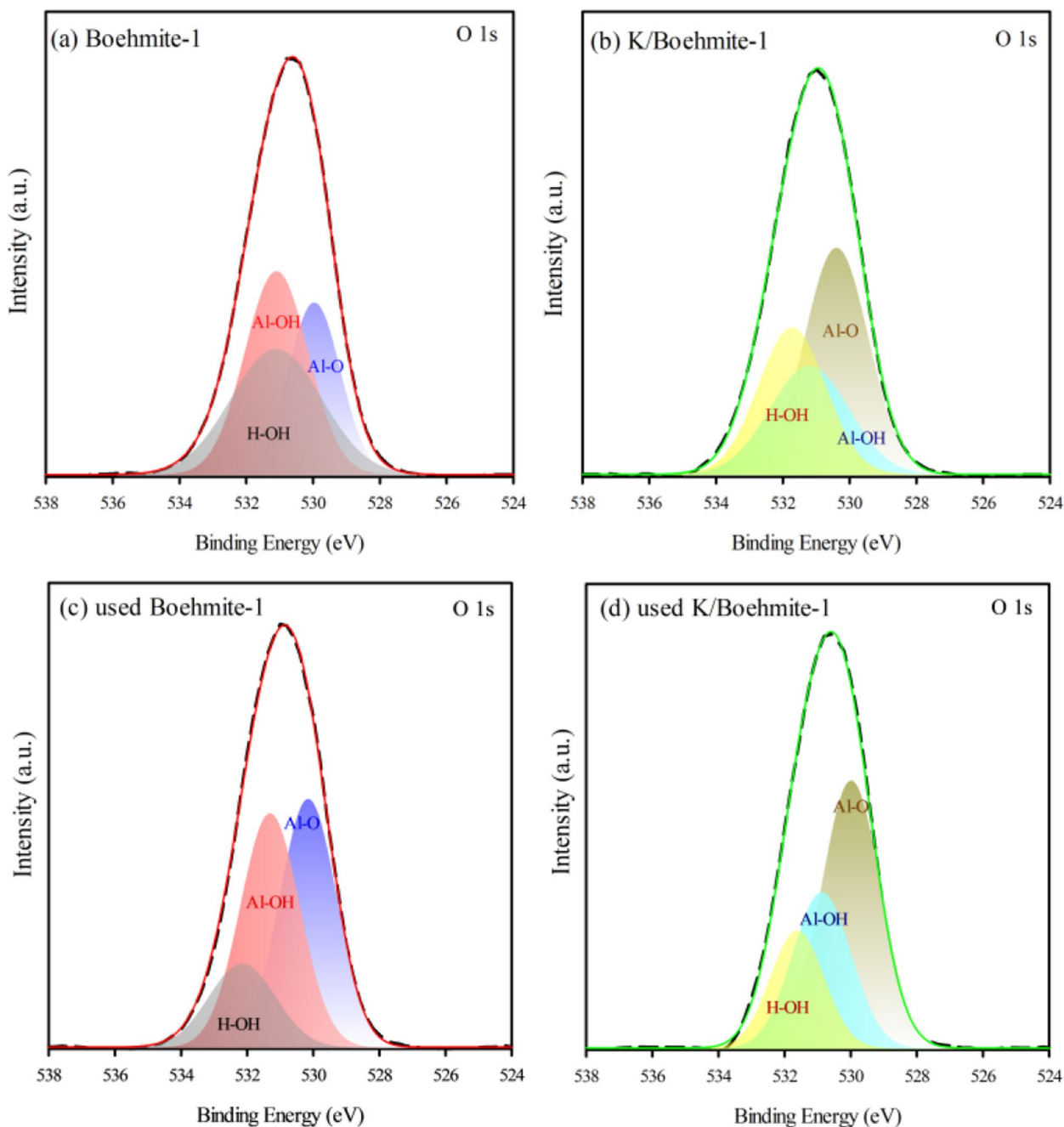


Fig. 10 XPS analysis of **a** fresh Boehmite-1, **b** K/Boehmite-1, **c** used Boehmite-1 and **d** used K/Boehmite-1 O1s

Table 3 Catalysts characterization by XPS

| | Al-O (%) | Al-OH (%) | H-OH (%) |
|-------------------|----------|-----------|----------|
| Boehmite-1 | 34.5 | 40 | 25.5 |
| K/Boehmite-1 | 43.9 | 26 | 30.1 |
| used Boehmite-1 | 39.4 | 41.4 | 19.2 |
| used K/Boehmite-1 | 50.6 | 29.2 | 20.2 |

between COS and K ions likely increases COS adsorption on the Al-based catalyst surface, providing more opportunities for COS to participate in the hydrolysis reaction. Subsequently, COS reacts with H₂O adsorbed on AlO(OH) via dissociated -OH groups to form CO₂ and H₂S. Thus, modifying with alkali metal hydroxide can increase -OH group amounts and enhance COS adsorption simultaneously. The possible hydrolysis

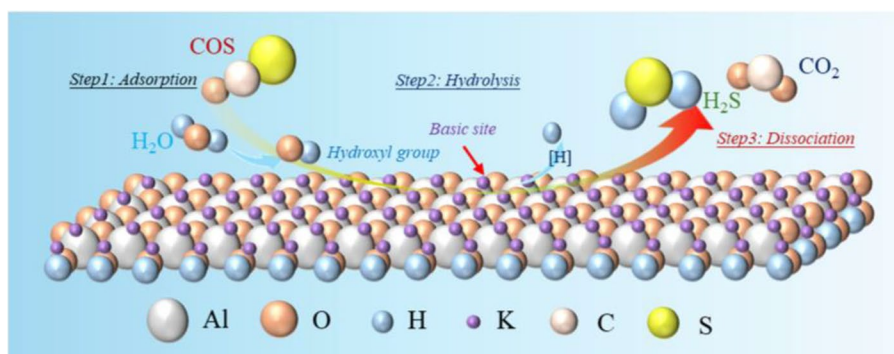


Fig. 11 Reaction mechanism of COS catalytic hydrolysis to produce H₂S using K/Boehmite materials

reaction path of COS occurring on the catalyst surface is shown in Fig. 11.

4 Conclusions

In this study, the alkali metal-treated boehmite catalysts exhibited markedly higher COS conversion efficiencies and H₂S yields across various temperatures compared to untreated boehmite. Notably, at 40 °C, COS conversion efficiencies for K/Boehmite materials were approximately 80%, with H₂S yields around 5–10%. At elevated temperatures (50, 60, and 70 °C), COS conversion approached nearly 100%, and H₂S yields significantly increased, reaching up to 98% for K/Boehmite-3. Furthermore, the introduction of KOH increased the number of active sites on the catalyst surface, as evidenced by the XPS analysis. These active sites facilitated the adsorption and reaction of COS, enhancing both conversion efficiency and H₂S yield. The alkali metal loading also promoted the formation of weak and medium basic sites, which are beneficial for the catalytic hydrolysis reaction. This study proposes a simple method for loading alkali metal onto boehmite, which significantly enhances its catalytic performance for the hydrolysis of COS, making it a promising approach for effectively removing COS in industrial applications. Additionally, the method can efficiently produce H₂S, which can be recycled for industrial processes, thereby achieving the goals of a circular economy.

Supplementary Information

The online version contains supplementary material available at <https://doi.org/10.1186/s42834-025-00242-4>.

Supplementary Material 1.

Acknowledgements

In addition, the authors would like to greatly thank Prof. Kun-Yi Andrew Lin for kindly providing analytical instruments and technical support to complete this research. We also extend our gratitude to The Instrument Center of National Chung Hsing University for their assistance with SEM, XRD, and XPS measurements.

Authors' contributions

Chih-Ying Wang facilitates on the formal analysis. Jia-Yu Lee carried out the methodology and investigation of this research. Jia-Yin, Lin participated in conceptualization, writing and supervision.

Funding

No funding was received.

Data availability

All data generated or analyzed during this study are available upon request to the corresponding author.

Declarations

Competing interests

The authors declare they have no competing interests.

Received: 1 July 2024 Accepted: 10 February 2025

Published online: 20 February 2025

References

- Zhao S, Kang D, Liu Y, Wen Y, Xie X, Yi H, et al. Spontaneous formation of asymmetric oxygen vacancies in transition-metal-doped CeO₂ nanorods with improved activity for carbonyl sulfide hydrolysis. *ACS Catal.* 2020;10:11739–50.
- Zhao S, Yi H, Tang X, Gao F, Yu Q, Wang J, et al. The regulatory effect of Al atomic-scale doping in NiAlO for COS removal. *Catal Today.* 2020;355:415–21.
- Shen L, Wang G, Zheng X, Cao Y, Guo Y, Lin K, et al. Tuning the growth of Cu-MOFs for efficient catalytic hydrolysis of carbonyl sulfide. *Chinese J Catal.* 2017;38:1373–81.
- Kim J, Do JY, Nahm K, Park NK, Chi J, Hong JP, et al. Capturing ability for COS gas by a strong bridge bonding of a pair of potassium anchored on carbonate of activated carbon at low temperatures. *Sep Purif Technol.* 2019;211:421–9.
- Kamp E, Thielert H, von Morstein O, Kureti S, Schreiter N, Repke JU. Investigation on the simultaneous removal of COS, CS₂ and O₂ from coke oven gas by hydrogenation on a Pd/Al₂O₃ catalyst. *Catal Sci Technol.* 2020;10:2961–9.
- Yu J, Lu Y, Wang S, Xu M, Jin Q, Zhu C, et al. Catalytic hydrolysis of carbonyl sulfide in blast furnace gas over Sm-Ce-O_x/ZrO₂ catalyst. *RSC Adv.* 2024;14:3135–45.
- Gu JN, Liang J, Hu S, Xue Y, Min X, Guo M, et al. Enhanced removal of COS from blast furnace gas via catalytic hydrolysis over Al₂O₃-based catalysts: Insight into the role of alkali metal hydroxide. *Sep Purif Technol.* 2022;295:121356.
- Yi H, Du C, Zhang X, Zhao S, Xie X, Miao L, et al. Inhibition of CO in blast furnace flue gas on poisoning and deactivation of a Ni/activated carbon catalyst in COS hydrolysis. *Ind Eng Chem Res.* 2021;60:18183–93.

9. Zhao S, Yi H, Tang X, Kang D, Wang H, Li K, et al. Characterization of Zn–Ni–Fe hydrotalcite-derived oxides and their application in the hydrolysis of carbonyl sulfide. *Appl Clay Sci.* 2012;56:84–9.
10. Li K, Liu G, Wang C, Li K, Sun X, Song X, et al. Acidic and basic groups introducing on the surface of activated carbon during the plasma-surface modification for changing of COS catalytic hydrolysis activity. *Catal Commun.* 2020;144:106093.
11. Qiu J, Ning P, Wang X, Li K, Liu W, Chen W, et al. Removing carbonyl sulfide with metal-modified activated carbon. *Front Env Sci Eng.* 2016;10:11–8.
12. Mohammadi M, Khodamorady M, Tahmasbi B, Bahrami K, Ghorbani-Choghmarani A. Boehmite nanoparticles as versatile support for organic–inorganic hybrid materials: Synthesis, functionalization, and applications in eco-friendly catalysis. *J Ind Eng Chem.* 2021;97:1–78.
13. Wei Z, Zhang X, Zhang F, Xie Q, Zhao S, Hao Z. Boosting carbonyl sulfide catalytic hydrolysis performance over N-doped Mg–Al oxide derived from MgAl-layered double hydroxide. *J Hazard Mater.* 2021;407:124546.
14. Zhao S, Tang X, He M, Yi H, Gao F, Wang J, et al. The potential mechanism of potassium promoting effect in the removal of COS over K/NiAlO mixed oxides. *Sep Purif Technol.* 2018;194:33–9.
15. Cao R, Wang L, Wang X, Xie Y, Li X, Ning P. Photothermal catalytic hydrolysis of COS with enhanced efficiency over constructed alkali-modified La–Ti catalyst: Adjusting photogenerated electron behavior through metal-support interactions. *Sep Purif Technol.* 2023;327:124884.
16. Song X, Ning P, Wang C, Li K, Tang L, Sun X, et al. Research on the low temperature catalytic hydrolysis of COS and CS₂ over walnut shell biochar modified by Fe–Cu mixed metal oxides and basic functional groups. *Chem Eng J.* 2017;314:418–33.
17. Wang X, Qiu J, Ning P, Ren X, Li Z, Yin Z, et al. Adsorption/desorption of low concentration of carbonyl sulfide by impregnated activated carbon under micro-oxygen conditions. *J Hazard Mater.* 2012;229–230:128–36.
18. Gao P, Li Y, Lin Y, Chang L, Zhu T. Promoting effect of Fe/La loading on γ -Al₂O₃ catalyst for hydrolysis of carbonyl sulfur. *Environ Sci Pollut R.* 2022;29:84166–79.
19. Zhang X, Zhou G, Wang M, Wang X, Jiang W, Zhou H. Performance of gamma-Al₂O₃ decorated with potassium salts in the removal of CS₂ from C₅ cracked distillate. *RSC Adv.* 2021;11:15351–9.
20. Cai Y, Huang H, Wang L, Zhang X, Yuan Y, Li R, et al. Facile synthesis of pure phase γ -AlOOH and γ -Al₂O₃ nanofibers in a recoverable ionic liquid via a low temperature route. *RSC Adv.* 2015;5:104884–90.
21. Song X, Sun L, Guo H, Li K, Sun X, Wang C, et al. Experimental and theoretical studies on the influence of carrier gas for COS catalytic hydrolysis over MgAlCe composite oxides. *ACS Omega.* 2019;4:7122–7.
22. Hu S, Gu JN, Li K, Liang J, Xue Y, Min X, et al. Boosting COS catalytic hydrolysis performance over Zn–Al oxide derived from ZnAl hydrotalcite-like compound modified via the dopant of rare earth metals and the replacement of precipitation base. *Appl Surf Sci.* 2022;599:154016.
23. Klopogge JT, Duong LV, Wood BJ, Frost RL. XPS study of the major minerals in bauxite: Gibbsite, bayerite and (pseudo-)boehmite. *J Colloid Interf Sci.* 2006;296:572–6.

Publisher's Note

Springer Nature remains neutral with regard to jurisdictional claims in published maps and institutional affiliations.